Polymer Chemistry

Anionic Polymerization and Transport of Diethyl Methylidene Malonate on Polyolefin Copolymer Surfaces

Journal:	*Polymer Chemistry*
Manuscript ID	PY-ART-05-2023-000506.R1
Article Type:	Paper
Date Submitted by the Author:	15-Jul-2023
Complete List of Authors:	Rehmann, Kelsi; University of Massachusetts Amherst, Chemical Engineering Klier, John; University of Massachusetts Amherst, Chemical Engineering Schiffman, Jessica; University of Massachusetts Amherst, Chemical Engineering

ARTICLE

Anionic Polymerization and Transport of Diethyl Methylidene Malonate on Polyolefin Copolymer Surfaces

Received 00th January 20xx,
Accepted 00th January 20xx

DOI: 10.1039/x0xx00000x

Kelsi M.S. Rehmann,[a] John Klier [a] and Jessica D. Schiffman *[a]

Polymer coatings are increasingly applied to polymeric substrates to improve interfacial properties in high wear environments. Thus, there is a need for chemically grafted coatings synthesized under practical conditions. Here, we explored methylidene malonates chemically grafted to commodity polymeric substrates with small amounts of nucleophilic initiator in the backbone. The polymerization and grafting conditions were evaluated by polymerizing diethyl methylidene malonate monomer (DEMM) from poly(ethylene-co-acrylic acid) (pEAA), both the acid form and the sodium salt, with varying concentrations of acrylic acid. For the first time, grafting of pDEMM was demonstrated on the substrates containing carboxylic acid and carboxylate salts using attenuated total reflectance Fourier transform infrared spectroscopy (ATR-FTIR). By studying the increase in monomer droplet area against a non-reactive control, we determined that the transport phenomena were reaction mediated and resulted in heterogenous amounts of grafted polymer. The area change over time was linear or stagnant at the beginning of the reaction (< 30 min), and the slope increased with increasing initiator for the base treated samples (between 0.01-0.03 cm^2/min). A heat map was constructed from ATR-FTIR spectra, which suggests heterogenous grafting on pEAA with 10% acrylic acid and the sodium salt of pEAA with 10% acrylic acid, and homogenous grafting on the sodium salt of pEAA with 3% acrylic acid. By understanding the transport and homogeneity of grafted pDEMM, we can optimize the covalent attachment of methylidene malonate polymers, which holds potential to increase the adhesion and durability of coatings.

Introduction

Many applications require stable and durable coatings to prevent delamination in high-wear environments, such as micro-electronics, aviation, and biomedical devices.[1,2] For example, in 2015, a safety communication issued by the United States of America's Federal Drug Administration reported that particulates, which were detaching from catheter coatings were causing blockages in patients' bloodstreams.[3,4] The state of the art technology in commercial biomedical coatings uses free radical polymerization and radical combination to covalently attach coatings to surfaces. Specifically, benzophenone-derivatives activated by ultra-violet light create radical species in the coatings and on the surface of polymeric medical devices through hydrogen abstraction; the radicals recombine and covalently bind the coating to medical devices and create crosslinks between the coating molecules.[5–9] While the benzophenone-based chemistry is effective, it is difficult to control as the benzophenone group produces both crosslinks and grafting sites. Additionally, the surface and polymer radical formation processes are inefficient, as hydrogen abstraction likely occurs with the solvent and other labile hydrogens.

Recent work has shown that methylidene malonates, a class of 1,1-disubstitued alkene monomers, are capable of anionic polymerization from carboxylate salts (**Scheme 1**) under ambient conditions.[10,11] Since small amounts of carboxylic acid and carboxylates are in the backbone of commercial polymers, such as Primacor and Surlyn, we hypothesize that methylidene malonates can be polymerized from readily available and commercial substrates with carboxylate salts or other common nucleophiles incorporated in the backbone, opening new avenues for facile bonding of coatings to surfaces.[12,13] Furthermore, a wide range of different functionalized groups can be incorporated into methylidene malonate polymers via esterification of the side chains or by using different starting malonates in the monomer synthesis, such as cyclic groups (e.g. ethyl cyclohexyl malonate), longer chain hydrocarbons, and vinyl groups (e.g. methylidene malonate-hydroxyethyl methacrylate).[14,15] The versatility of methylidene malonate chemistry shows promise as coatings for biomedical devices or tie layers for commercial coatings.

A shortcoming of traditional anionic polymerization is that it employs highly reactive anionic initiators, such as butyl lithium, and requires stringent reaction conditions, due to premature termination by air and water. The anionic polymerization of methylidene malonates can be initiated by a variety of simple nucleophiles in the presence of water and oxygen, including

[a] Department of Chemical Engineering, University of Massachusetts Amherst, Amherst, Massachusetts 01003-9303.
*Corresponding author: Jessica D. Schiffman; Email: schiffman@umass.edu
Electronic Supplementary Information (ESI) available: ATR-FTIR by peak fitting and ratios of peak areas, representative peak fitting with MATLAB, adsorption vs surface initiated grafting experiments, replicate spectra for front and back of film after grafting, heat map values for polymerization and grafting data, schematic of reactive-transport mechanism
See DOI: 10.1039/x0xx00000x

carboxylate salts, hydroxides, and phenol salts. Additionally, methylidene malonate polymerized from tertiary amines can yield high molecular weight polymers at room temperature.[11] However, methylidene malonates may also undergo Michael addition in the presence of electrophiles, producing a small molecule species and preventing monomers from participating in polymerization. With this combination of robust polymerization and accessible initiating groups, the reactivity of methylidene malonates may enable *in situ* grafting of polymer coatings to polymer surfaces under a wide range of scalable conditions.

Beyond methylidene malonates, other atypical chemistries and initiators have been used to induce room temperature anionic polymerization. Cyanoacrylates, commercially known as super glue, polymerize through a similar anionic mechanism[16] and have widespread use in consumer applications due to their polymerization from surface water. Cyanoacylates are limited in their ability to polymerize on porous surfaces and in the presence of weak acids: carboxylic acid in particular is a known chain transfer agent.[17] The high reactivity of cyanoacrylates also leads to highly sensitive initiation, difficulty in measuring reliable polymer kinetics, and broad polydispersity (e.g. Đ=2.14).[16,18,19] Another approach to room temperature anionic polymerization utilizes exotic initiators, which are capable of initiating more common monomers. When used to polymerize methyl methacrylate, tetrabutyl ammonium salts of CH acidic compounds have discrepancies between calculated and experimental M_n, display an induction time (i.e., initial polymerization delayed), low yield, high polydispersity, and incomplete initiation consumption (i.e., slow initiation).[20–22]

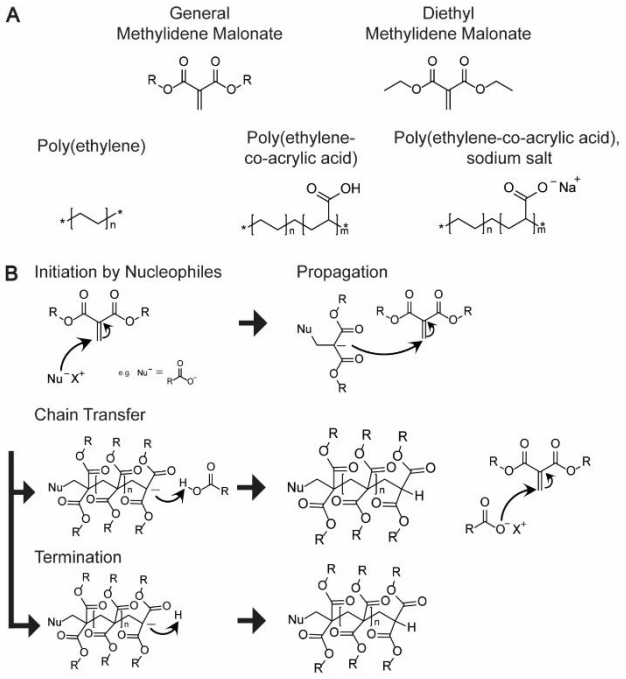

Scheme 1. Heterogenous polymerization of methylidene malonates on poly(ethylene) and poly(ethylene-co-acrylic acid) substrates. (A) Chemical structures of generic methylidene malonate and the specific methylidene malonate used for this study, diethyl methylidene malonate. The substrates used in this study include poly(ethylene), poly(ethylene-co-acrylic acid), and poly(ethylene-co-acrylic acid), sodium salt. (B) Anionic polymerization mechanism generalized for methylidene malonate, including termination and chain transfer steps.

Reetz et al. [21] reported that there was an induction period because the initiation was slower than the propagation. Other exotic initiators include tetrabtyl ammonium salts of thiourea compounds, which seem to share similar limitations (e.g., high Đ, slow initiation).[23] Although these tetrabutyl ammonium salts showed promising results for some monomers, these initiators are not functionalities that are common in the backbone of commercial polymers; they may be difficult to incorporate into a substrate as an initiator due to the use of organic solvents to create the salt from the acid. Unlike cyanoacrylates, methylidene malonates have been shown to produce narrower weight distributions (Đ=1.63 compared to 2.14), better biocompatibility, and more controlled reactivity (less sensitive to moisture for example).[16,24,25] Some reversible-deactivation radical polymerization schemes can occur in the presence of oxygen or air, but usually require elevated temperatures, mitigation of moisture, and/or complicated processes to graft initiators to the substrate prior to polymerization.[26–29] Thus, this study evaluates the grafting and polymerization of methylidene malonates under practical conditions, i.e., in the presence of air and water.

Here we explore methylidene malonate polymerization initiated and grafted on a commodity polymer film, poly(ethylene-co-acrylic acid) (pEAA). pEAA contains a high concentration of ethylene groups that are difficult to functionalize (>80% of the copolymer) and a small amount of acrylic acid groups (3-10 mol%), which are neutralized to carboxylate salts (e.g., initiators for methylidene malonates) with base treatment. The surface-initiated polymerization and grafting of diethyl methylidene malonate from these substrates are studied in ambient conditions (e.g., in the presence of air and water). Here, we observe the effects of monomer transport on the surface polymerization and describe the relationship between the transport of monomer and subsequent grafting to polymer substrates. We suggest methylidene malonate monomers enable grafting to complex surfaces under ambient conditions and hold potential for facile application at industrial scale.

Experimental

Materials and Chemicals.

Low density polyethylene (LDPE) pellets, sodium hydroxide, 1,1,3,3-tetramethyl guanidine (TMG), and trifluoracetic acid (TFA) were purchased from Sigma Aldrich. Poly(ethylene-co-acrylic acid) (EAA) was supplied by Dow and SK Global Chemicals via their distributor, Entec, as commercial resin pellets with 9.8 wt% acrylic acid content, Primacor 1410 (pEAA-10), and 3 wt% acrylic acid content, Primacor 3150i (pEAA-3). Diethyl methylidene malonate (DEM=M) was provided by Sirrus, Inc. Chloroform and dichloromethane were purchased from Fischer Scientific. Diethyl methylmalonate (DEM-M) and tetrahydrofuran (THF) were purchased from Tokyo Chemical Industry (TCI Chemicals). Deionized (DI) water was acquired either by reverse osmosis filtering of house water or Millipore filtering of water with a resistivity of ~ 18 mega-ohms/cm.

Preparation of Non-base Treated and Base Treated Films.

All polymer films were fabricated with a Carver Bench Top Manual Laboratory Hydraulic Press with heated platens. A stainless-steel block with dimensions of 15.24 x 15.24 cm was covered by a 0.0051 cm thick film of Kapton (McMaster Carr), and a 0.075 x 8.0 x 11 cm (thickness x length x width) metal frame was placed on top of the Kapton film. Eight grams of polymer pellets were added into the frame, covered with another sheet of Kapton film, and covered with a second stainless-steel block. The system was placed on the bottom platen of the press and the temperature was set to 150-160°C. A nominal pressure of ~50-150 lbf was applied, and the films were pre-melted for 3 min. Approximately 1500 lbf was applied, and the films were pressed for 5 min. Films were cooled by holding the stainless-steel assembly so that the metal plate was in contact with the surface of a room temperature water bath for 3 min total, cooling for 30 s on each side. Throughout the results section, films that were directly cut from the melt pressed films will be referred as "non-base treated samples" and abbreviated as LDPE for low density poly(ethylene) films, pEAA-3 for poly(ethylene-co-acrylic acid) with 3 mol% acrylic acid, and pEAA-10 for poly(ethylene-co-acrylic acid with 10% acrylic acid.

The base treatment consists of the following steps. The melt pressed films were cut (5.5 x 1.5 cm) and submerged in 35 mL of 0.1 N sodium hydroxide in a 50 mL conical tube. The conical tube was added to an orbital rotating plate (CO-Z) at 100 rpm for 24 hr. After removal from the base treatment, the films were blotted dry with a Kimwipe and cut into square samples (1.5 x 1.5 cm). Base treated samples will be referenced as LDPE-Na for low density poly(ethylene) films, pEAA-3-Na for base treated poly(ethylene-co-acrylic acid) films with 3 mol% acrylic acid, pEAA-10-Na for base treated poly(ethylene-co-acrylic acid) films with 10 mol% acrylic acid.

Polymerization of Methylidene Malonate Monomers on Polyolefin Films.

Substrates (1.5 x 1.5 cm) for surface initiation were cut from either the melt pressed (non-base treated) or from the base treated films, and their mass was determined using a Mettler Toledo AX105DR analytical balance. Diethyl methylidene malonate (5 µL) was added to the surface of the films, which were left to react for 24 hr at room temperature in ambient conditions within a closed poly(styrene) dish to prevent monomer evaporation.

Washing of Non-grafted Polymer from Film Substrate.

To remove non-grafted polymers, each substrate with polymerized diethyl methylidene malonate was submerged in 20 mL of chloroform and placed on an orbital rotating plate for 48 hr at 100 rpm. The removed films were dried in a chemical hood at room temperature for ~ 72 hr before analysis.

Polymerization of Methylidene Malonate Monomers in Solution.

DEM=M monomers were polymerized in a THF solution to determine the chemical spectra of pDEMM, which was used as a control for the determination of grafted pDEMM in the surface initiation experiments. In a 50 mL flask, a stir bar and 10 mL of THF were added at room temperature (no heat control or water bath); TMG was diluted in THF and 2×10^{-5} mol TMG was added to the flask and stirred under nitrogen. After sufficient nitrogen moved through the system, 1.0 g of DEMM was added by syringe. After 1 hr, excess TFA was added to quench the reaction. The solvent was removed by vacuum distillation at room temperature; no further purification was conducted.

Chemical Characterization using FTIR Spectroscopy.

The surface chemistry of the films was determined using the Attenuated Total Reflectance (ATR) attachment on a Bruker Alpha Spectrophotometer with a diamond crystal. Samples were scanned from 4000-400 cm^{-1} with 24 scans per experiment and 4 cm^{-1} resolution. With an approximate refractive index of 1.5, the sample depth measured was between 0.5-5.0 µm. To analyze the peak areas, the Bruker files (.JCAMP) were imported to MATLAB (version R2021a), and fit with multiple Lorentzian peaks using the peakfit program.[30] A detailed description of the analysis is in the Electronic Supplementary Information and **Figure S1**.

Characterization of Liquid Transport by Area Measurements.

Digital images were captured using a Samsung Galaxy S10e during polymerization and analyzed with *ImageJ* software version 1.50i.[31] An outline of the film substrate area was created with the Polygon selection tool whereas the methylidene malonate droplet progression was outlined using the freehand selection tool. The film area and the methylidene malonate outline were calculated with the Measure function in *ImageJ*. To correct for slight angle variations, the area of the front calculated by *ImageJ* was multiplied by the ratio of the area of the film (2.25 cm^2) and divided by the area of the film measured in *ImageJ*.

Statistical analysis was completed using ANOVA with Tukey-Kramer HSD test on the replicates (n=3) of individual time points for each substrate-liquid combination (8 pairs) and compared across all pairs using JMP ($p< 0.05$). Calculations of slope were measured by defining slices of time between induction time (0 or 10 min) and the end of the linear region (30 min) and using the linear regression tool in Origin to create a best fit line of the corrected area as a function of time.

Result and Discussion

Surface-Initiated Polymerization of Methylidene Malonates.

The polymerization of diethyl methylidene malonate (DEM=M) was investigated on three polyolefin surfaces: low density polyethylene (LDPE, no initiator in the polymer backbone), poly(ethylene-co-acrylic acid) with 3% acrylic acid content (pEAA-3, low levels of initiator), and poly(ethylene-co-acrylic acid) with 10% acrylic acid content (pEAA-10, high levels of initiator) (**Figure 1**). Polymerization in air at room

temperature was tested on each substrate under two conditions: with or without sodium hydroxide treatment. The sodium hydroxide treatment converts surface carboxylic acid species into nucleophilic, carboxylate salts. Pure monomer, without dilution in solvent, was used because solvents can change the nucleophilicity of both the initiator and the growing chain end, thereby influencing the rate of initiation and propagation of the polymerization.[32,33] After polymerization for 24 h, the methylidene malonate was mostly solid with heterogenous levels of opacity on all films; in some cases, tacky liquid was observed, which visually suggested polymerization (**Figure 1B**).

On the LDPE-Na substrates, we observed hazy, ring-like areas of polymer emanating from a central circle with decreasing levels of opacity from the center to the edge; the central circle was the same size as the monomer droplet. These observations suggest that the monomer moved slowly out from the center. On pEAA-3-Na, hazy polymer layers covered the full film surface with some opaque (nearly white) polymer flakes interspersed. The pEAA-10 substrate exhibited a completely opaque polymer circle in the sample center, with similar dimensions to the original monomer droplet. The area outside of the circle was more translucent than the original pEAA-10 film, suggesting a thin layer of pDEMM. pEAA-10-Na substrates displayed a center polymer circle of mixed opacity, surrounded by a "ring" of completely opaque polymer; the sections outside of this circle vary in opacity and translucency. On all substrates, the polymerized diethyl methylidene malonate (pDEMM) occupied a larger area than the initial monomer droplet; in some cases, polymer was found on the bottom side of the film.

To understand these observations, we considered the relationship between wetting and substrate chemistry. The addition of carboxylic acids to the surface of poly(ethylene) can decrease the water contact angle significantly, indicating higher hydrophilicity: previous work has shown that when poly(ethylene) is oxidized to contain a mixture of ketone, aldehyde, and carboxylic acid groups (with ~30% carboxylic acid) the contact angle decreased to ~50°, compared to ~100°C for neat poly(ethylene).[34,35] In the same work, the contact angle additionally decreased when basic water was used (contact angle ~ 20°, pH > 12). Therefore, we expect that the acrylic acid copolymer films will have a slight increase in hydrophilicity compared to poly(ethylene), and the neutralized copolymer films will have a further increase in hydrophilicity, even though the amount of total acrylic acid is small (<10 %). On the surface, there may be a significant amount of carboxylate compared to the bulk; it has been hypothesized that pEAA becomes more hydrophilic when immersed in a buffer solution, as the surface can rearrange to present acrylic acid groups.[13] Due to the polar structure of DEM=M, we expect increasing hydrophilicity to correlate with more favorable interactions between the reacting group and surface.

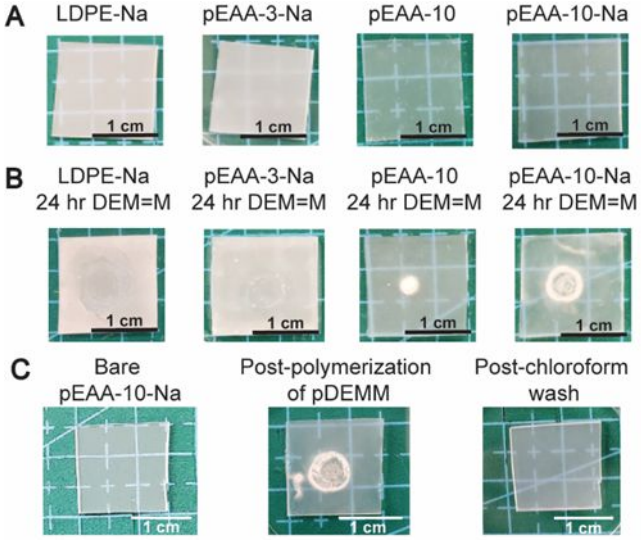

Figure 1. Representative digital photographs of base treated substrates (LDPE-Na, pEAA-3-Na, and pEAA-10-Na) and an acrylic acid substrate (pEAA-10) (A) before and (B) after 24 hr polymerization with DEM=M. (C) Representative digital photographs of a pEAA-10-Na substrate after base treatment; after 24 hr polymerization of diethyl methylidene malonate, and after being washed with chloroform.

Wetting can be a complex phenomenon based on the balance of surface tension between the liquid, solid, and vapor phases, as well as the roughness and porosity of the surface.[36] In simple wetting without reaction, we would expect the DEMM liquid to create a new interface as the liquid drop comes into contact with the solid, and initially spread to an equilibrium value within a few minutes at a rate of $1/t^{\kappa}$, in which κ is 0.1 for a smooth surface and increases with surface roughness, depending on model assumptions.[36–38] Spontaneous spreading, in which the liquid has a contact angle of 0°, can be pinned by heterogeneities or roughness of the surface. Coffee rings, for instance, are caused by the pinning of the liquid interface by particles, which results in a flow toward the pinned interface as the liquid evaporates.[36,39] The presence of coffee rings in **Figure 1**, despite the evaporation being minimized by covering the system, and the increase in area beyond the first few minutes, suggest a more complex phenomenon than simple wetting. From these initial observations, two major questions arose: i) was the polymerized diethyl methylidene malonate grafted to the surface and ii) how were the diethyl methylidene malonate molecules migrating during polymerization?

Assessing Grafted Poly(Diethyl Methylidene Malonate) using ATR-FTIR.

Polymerization of methylidene malonates from polymer surfaces is difficult to characterize because common surface techniques, such as ellipsometry and atomic force microscopy are typically conducted on hard substrates (such as silicon wafers or mica) and are not suitable on our thick heterogeneous samples. We attempted to cleave the poly(diethyl methylidene malonate) from the substrate using acid ethanolysis (to prevent unwanted cleavage of the diethyl side chains), however, according to our ATR FTIR analysis, pDEMM remained present after almost 30 hours of exposure at elevated temperatures. The determination of molecular weight using gel permeation chromatography (GPC) and matrix-assisted laser deposition and ionization time of flight mass spectroscopy (MALDI-TOF MS) of solution based, high molecular weight poly(methylidene malonates) (pMM) presented additional challenges, such as the polymer's poor solubility in common GPC mobile phases. Preliminary MALDI-TOF measurements acquired on solution polymerized pDEMM showed lower molecular weights than expected, likely due to the broad polydispersity of the pDEMM and chain transfer with ambient water. Due to these complications, we determined that ATR-FTIR, a semi-quantitative method, was the most suitable to characterize

poly(methylidene malonates) that was grafted onto thick polymer films.

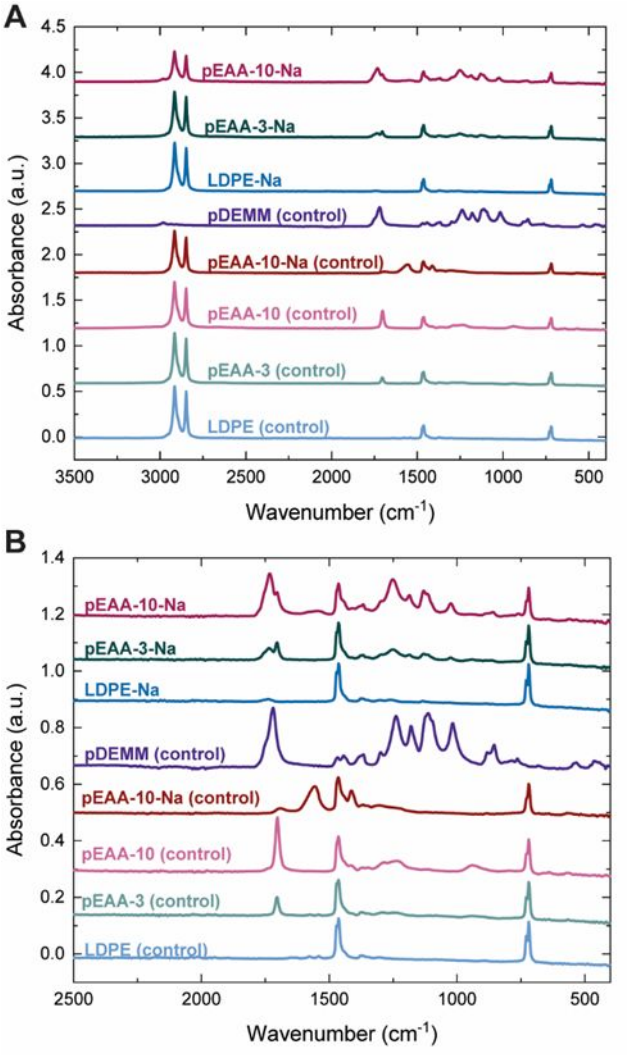

Figure 2. ATR-FTIR spectra confirm the grafting of poly(diethyl methylidene malonate) to base treated polyolefin substrates. Representative (A) spectra and (B) insets highlight the carbonyl and fingerprint regions and confirm the presence of pDEMM on the three substrates. From bottom-to-top in (A) and (B): three control polyolefin substrates without base treatment or addition of DEM=M; pEAA-10-Na to demonstrate the shift of the carboxylic acid peak to lower wavenumbers, signifying the presence of the carboxylate salt; pDEMM control, diethyl methylidene malonate polymerized in solution. In the top three spectra (labelled with the base treated substrates LDPE-Na, pEAA-3-Na, and pEAA-10-Na), diethyl methylidene monomer was polymerized on the substrate and washed of non-grafted polymer. Poly(diethyl methylidene malonate) is present on all three base treated substrates.

To determine if poly(diethyl methylidene malonate) was grafted to the surfaces, the substrates were exposed to excess chloroform to remove non-grafted pDEMM. After exposure to chloroform, pDEMM was not observed on the substrates visually (**Figure 1C**). Carbonyls, such as the esters of pDEMM, result in high intensity bands in the mid-IR region; thus, ATR-FTIR can detect the presence of pDEMM. However, the carboxylic acid peaks of the pEAA substrate can potentially overlap with the ester peaks of pDEMM. By comparing the spectra of the initial film substrates to solution polymerized pDEMM, we identified distinct spectral signatures of pEAA and pDEMM (**Figure 2**). In the hydrocarbon region, pEAA exhibits two peaks at 2916 and 2848 cm^{-1} correlating to the methylene asymmetric and symmetric stretches, respectively.[40] In comparison, pDEMM has four hydrocarbon peaks at 2980, 2937, 2904, and 2875 cm^{-1}, with the peak intensities decreasing as the wavenumber decreases.[40] The peaks represent the methyl asymmetric stretch, the methyl symmetric stretch, the methylene asymmetric stretch, and the methylene symmetric stretch, respectively. In the hydrocarbon region of the spectra, the most intense peak for pDEMM occurs at higher wavenumbers compared to the peaks for pEAA.

The main carbonyl peaks are between 1500-1800 cm^{-1}: for pEAA, this peak is between 1690-1705 cm^{-1} for the carboxylic acid and ~1556 cm^{-1} for the carboxylate salt (when base treated).[40] The range listed for the carboxylic acid peak (~1700 cm^{-1}) indicates the presence of acid dimers; free acids are associated with peaks at higher wavenumbers (~1750 cm^{-1}) for poly(ethylene-co-methacrylic acid), and the same shift is expected for pEAA.[41,42] In this work, we were also concerned with comparing the acid peak to the carboxylate salt and the ester carbonyl peaks, so although the COOH is likely in the dimer state, this peak will be referenced as the carboxylic acid peak. The main pDEMM carbonyl peak occurs at 1719 cm^{-1} in the control sample with a shoulder at 1745 cm^{-1}. Both peaks are distinct from the carbonyl peaks for the polyolefin substrates, as evident by the ~10-15 cm^{-1} shift of the main peak and the differences in the peak shapes.[40,43] Thus, we can differentiate from the pDEMM ester carbonyl and the pEAA carboxylic acid carbonyl.

While the region from 1000-1500 cm^{-1} is complex,[40] a third, unique pDEMM fingerprint is present with four distinct peaks at 1239, 1181, 1113, and 1018 cm^{-1}. The asymmetric stretches of the bonded atoms on either side of the ester oxygen are likely between 1300-1000 cm^{-1}. Specifically, the asymmetric C-C-O stretch is near 1200 cm^{-1} and the asymmetric O-C-C stretch is near 1100 cm^{-1}.(34) Notably, these four peaks appear in the spectra of the pDEMM control and are not present in the pEAA or LDPE spectra, so we can use these peaks to identify pDEMM in subsequent studies.

Since the pDEMM spectra is distinct from pEAA, we can measure pDEMM grafting. Visually, the films appeared to have little pDEMM remaining after non-grafted polymer was removed: the opaque polymer was no longer present (**Figure 1**). ATR-FTIR analysis revealed that varying amounts of pDEMM were present on all substrates (**Figure 2**). On LDPE-Na, the pDEMM carbonyl peak was small or undetectable, which was

expected since LDPE does not contain any initiators for pDEMM in the polymer backbone. Three small peaks in the bare LDPE substrate were observed at 1646, 1577, and 1542 cm^{-1}, likely from a polyolefin additive containing secondary amides, which have strong N-H in plane bends from 1570 to 1515 cm^{-1} and a C=O stretch at 1630-1680 cm^{-1}.[40] Secondary amides with long olefin chains are used as slip agents in polyolefins, to reduce tackiness during molding and processing.[44] These secondary amides are unlikely to initiate DEM=M, but could act as chain transfer agents. In the case of the pEAA-3-Na substrate, two distinct peaks were observed at 1735 and 1704 cm^{-1}, representing the pDEMM and pEAA carbonyls, respectively. In the fingerprint region, peaks at 1250, 1185, 1129, and 1024 cm^{-1} confirmed the presence of pDEMM. In the case of pEAA-10-Na, a carbonyl peak at 1733 cm^{-1}, with a buried peak at 1704 cm^{-1}, demonstrated more pDEMM than pEAA was at the surface. However, we also note that the pEAA-10-Na substrates contained residual carboxylate functionality, so a definitive comparison cannot be made just by the relative peak areas of the acrylic acid carbonyls.

Substrates without base treatment (e.g., no carboxylate initiators) were studied as controls. After 24 hr, we observed polymerized DEMM, and after removing non-grafted polymer, pDEMM peaks were present in the pEAA-3 and pEAA-10 spectra (**Figure 3**). In the case of pEAA-3 and pEAA-10, the pDEMM carbonyl relative peak heights and peak areas were more intense than the pEAA carbonyl. In the fingerprint region, the four peaks associated with pDEMM were present. In the case of LDPE, some spectra included very small peaks for the pDEMM carbonyl; however, the presence of these peaks was less consistent than in the case of base treated LDPE. The presence of such intense pDEMM peaks was surprising, since the pEAA samples do not contain known initiators for methylidene malonates; carboxylic acid has significantly less nucleophilicity

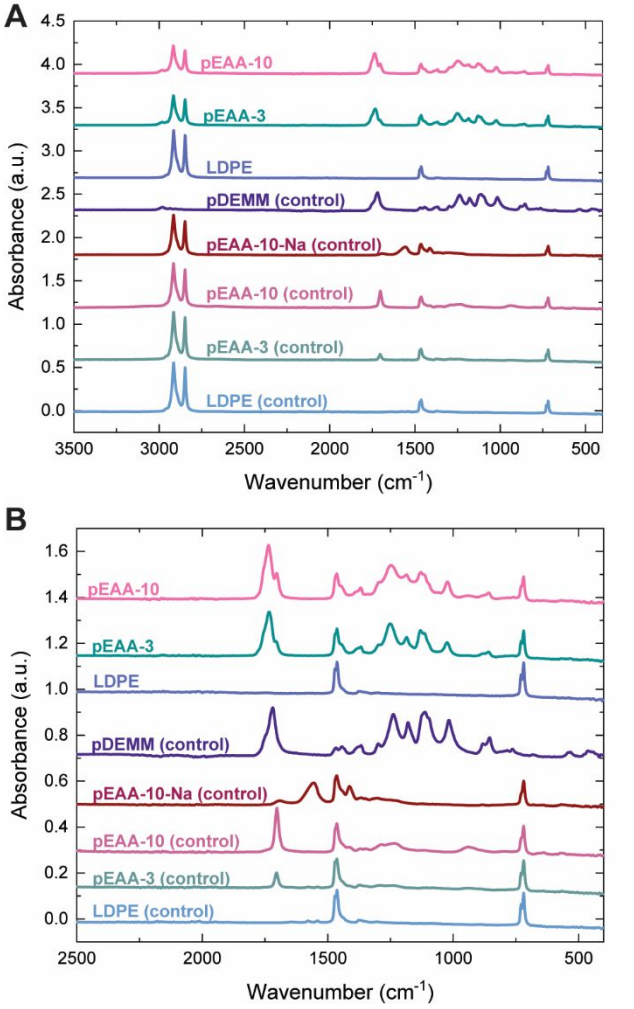

Figure 3. ATR-FTIR spectra confirm the grafting of poly(diethyl methylidene malonate) to polyolefin substrates without base treatment. Representative (**A**) spectra and (**B**) insets that highlight the carbonyl and fingerprint regions confirm the presence of pDEMM on the acrylic acid substrates. From bottom-to-top in (A) and (B) three control polyolefin substrates without base treatment; pEAA-10-Na demonstrating the shift of the carboxylic acid peak to lower wavenumbers, signifying the presence of the carboxylate salt; pDEMM control, diethyl methylidene malonate polymerized in solution. In top three spectra diethyl methylidene monomer was polymerized on the substrate and washed of non-grafted polymer. Poly(diethyl methylidene malonate) is present on the two acrylic acid containing substrates(pEAA-3 and pEAA-10) but not the pure polyolefin substrate (LDPE).

than the carboxylate salt and was not expected to initiate anionic polymerization. The substrates without base treatment could contain pDEMM if the DEMM polymerizes from surface water, similar to cyanoacrylates, the analogous class of 1,1-disubstituted alkenes mentioned in the introduction, and the carboxylic acid acts as a chain transfer agent.[17] However, the acidity of carboxylic acid is orders of magnitude higher than the acidity of water, making the dissociation of the carboxylic acid more likely than the dissociation of water. A simple explanation could be that some of the acid is dissociating into the carboxylate form and initiating polymerization, while the acidic proton is providing chain transfer. Another potential explanation is that the DEM=M polymerized from surface water and simply associated with the acrylic acid backbone strongly enough to prevent dissolution during the solvent wash (e.g., intermolecular bonding between the pDEMM carbonyl and backbone acidic hydrogen). Due to the extensive chloroform wash and low amounts of acrylic acid in the substrate, it is less likely that intermolecular bonding would be strong enough to anchor pDEMM to the surface.

Potentially, the pDEMM observed in all of these cases was due to physical adsorption, in which the pDEMM associated more strongly with as received pEAA, then neutralized pEAA, and not at all with LDPE. As previously mentioned, the substantive chloroform wash suggests that the pDEMM was anchored to the substrate by stronger bonds, e.g., carboxyl groups bond with the pDEMM. Some of our preliminary data, in which pDEMM was adsorbed to pEAA-10-Na in dichloromethane, revealed the presence of carboxylic acid carbonyls in similar proportions to the carbonyl in the bare substrate, see **Figures S2, S3,** and **S4**. However, in the case of pDEMM polymerized on pEAA-10-Na, the carboxylic acid carbonyl has a smaller peak height than the pDEMM carbonyl and a peak height in between the slightly neutralized and very neutralized pEAA-10-Na carbonyl peak. This suggests that more of the carboxylic acid carbonyl is consumed than can be accounted for by only neutralization in the "grafted" sample. Thus, it is suggested that carboxylic acid is consumed in the "grafted" sample and is not consumed in the adsorption case.

Preliminary studies were performed using diethyl methylidene malonate polymerized on LDPE, LDPE-Na, pEAA-10, and pEAA-10-Na under nitrogen within a glove box. In the LDPE with and without base treatment, the samples remained liquid, while on pEAA-10, the samples formed a slightly opaque film. The pEAA-10-Na samples had a clear film of pDEMM which overflowed, causing them to adhere to the poly(styrene) plate in which the experiment was conducted. Only the LDPE and pEAA-10 samples could be washed with solvent for comparison: the ATR FTIR spectra for the LDPE and LDPE-Na samples lacked the pDEMM peak, whereas the peak was present in the pEAA-10 samples. In the same study, DEMM polymerization of pEAA-10 was studied under air and under nitrogen: the normalized peak areas were approximately double under nitrogen than in air. However, in this study, we were most concerned with assessing the polymerization in facile processing conditions, so upon seeing similar samples within or outside of the glovebox, we focused on studying the films polymerized in ambient conditions.

Assessing Heterogeneity of Polymerization using ATR-FTIR.

While **Figures 2** and **3**, feature representative data, due to the visual heterogeneity (i.e., different patterns of opacities), we also acquired spectra at six distinct locations across the film (at the center and corners). The amount of pDEMM varied across the films and the spectral signature of pDEMM was also present on the underside of the film, suggesting that the methylidene malonate diffused through the polyolefin film (**Figure S5**). In **Figure 4**, a heat map is provided that represents the pDEMM spatial distribution after polymerization but before the solvent wash; each color block represents the average peak ratios of the pDEMM carbonyl peak and the methylene peak of the substrate (i.e., either LDPE or pEAA). In some experiments, the DEMM carbonyl peak or pEAA/LDPE methylene peak were not detected, and thus, in **Figures 4** and **5** black indicates the lack of substrate peak detection. In the LDPE-Na substrate, the center of the top of the film (near where the monomer droplet was deposited) had very little pDEMM while higher amounts of pDEMM were measured in the corners based on the disappearance of the substrate peaks. The FTIR data corroborates the visual observation in **Figure 1**, in which LDPE

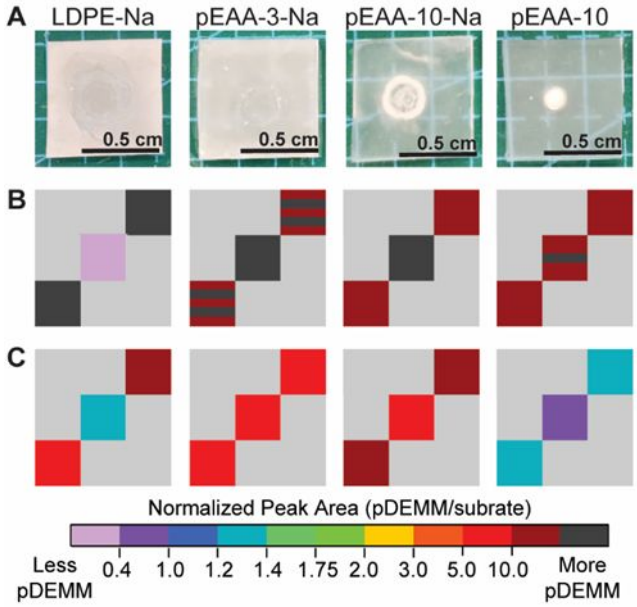

Figure 4. (A) Representative digital images of heterogenous polymerization of pDEMM on LDPE-Na, pEAA-3-Na, pEAA-10-Na, and pEAA. (B, C) The associated heat maps represent the amount of pDEMM on the (B) top and (C) bottom side of the sample after polymerization but before excess polymer was dissolved from the substate, acquired from the ATR-FTIR spectra. The normalized peak area was calculated using Equation S1. Table S1 provides the average and standard deviation of the normalized peak areas.

has rings of pDEMM around the center. The back side of the film had higher amounts of pDEMM at the corners and slightly less pDEMM at the center. In at least one replicate, pDEMM polymerized at the bottom edge where the substrate meets the poly(styrene) plate used to house the films, suggesting the DEM=M/pDEMM transported away from the center and over

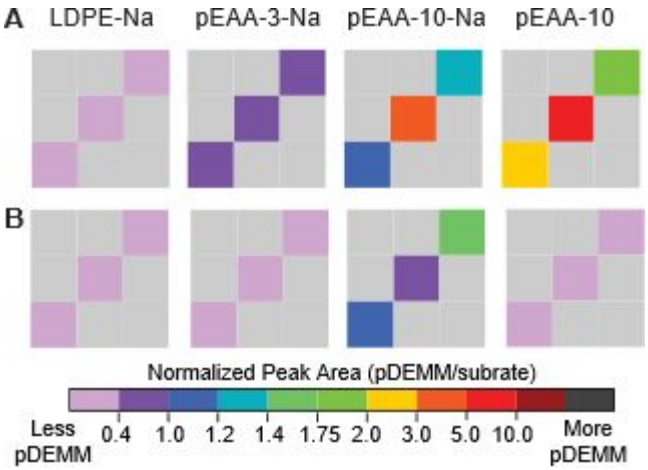

Figure 5. Heat maps representing the spatial distribution of grafted pDEMM on the surface after washing the non-grafted polymer. The associated heat maps represent the amount of pDEMM grafted on the (A) top and (B) bottom side of the sample acquired from the ATR-FTIR spectra taken after excess pDEMM was washed from the substrate with chloroform. The normalized peak area was calculated using Equation S1. Table S2 provides the average and standard deviation of the normalized peak areas.

the edges. We note that the films were not stuck to the poly(styrene) plates.

In the pEAA-3-Na samples, the center region on the top of the film had a very high relative pDEMM intensity and slightly lower intensity at the corners (**Figure 4,** column 2). In these samples, a significant amount of pDEMM resulted in peaks at 764 cm^{-1} (which are seen in the pDEMM control) that sometimes overlapped the substrate peaks at 719 cm^{-1}. In the top corners of pEAA-3-Na, the substrate peaks were visible in the spectra but not deconvoluted from the pDEMM peaks in the 700-800 cm^{-1} region, making it difficult to accurately calculate the peak area ratios. On the bottom of the film, there was less pDEMM than in the bottom of the LDPE films.

The pEAA-10-Na samples had more pDEMM detected in the center than at the sides of the top of the film; additionally, more pDEMM was detected at the sides of the bottom of the film than at the center (**Figure 4**, column 3). At least one replicate of this sample also had pDEMM pooled at the intersection of the edges of the film and the polystyrene plate. In the pEAA-10 sample, more pDEMM was in the center than on the edges (**Figure 4**, column 4). On the bottom side of the film, there was less pDEMM than in the pEAA-10-Na samples.

From the data in Figure 4, the largest concentration of pDEMM was in the center of the films containing COO-Na+ or COOH (i.e., pEAA-X), but not in the center for LDPE. The spectral signature of pDEMM was also detected on both sides of the film. There are, in some cases, pools of pDEMM on the edges. We hypothesize that the pDEMM moved through the film, because we did not observe pDEMM flowing over the sides and seeping underneath the film. We also note that there was less pDEMM on the bottom side of the films for samples without COO- Na+ (i.e., LDPE and pEAA-10); this may be because monomer preferentially polymerized at the top of the film, rather than moving through the film or across the sides.

Assessing Grafted Polymer Heterogeneity using ATR-FTIR.

To assess the grafting of pDEMM to polyolefin substrates, the same analysis was performed on samples after non-grafted polymer was removed with chloroform. The LDPE samples had a very small spectral signature of pDEMM (**Figure 5**, column 1). The negligible amount of grafted pDEMM on LDPE-Na was consistent with our understanding that LDPE does not contain any initiating species in the backbone. However, trace pDEMM could be seen, likely entangled in the substrate chains.

The pEAA-3-Na samples had grafted polymer on the top of the film and very little to no pDEMM on the bottom of the film. The heat map values of 0.4-1.0 (dark purple) are associated with a slightly less intense pDEMM peak than the remaining, unreacted carbonyl peak of the substrate. The grafted pDEMM distribution was quite homogenous on the top of the pEAA-3-Na substrates.

The pEAA-10-Na samples had the highest intensity pDEMM signal at the center of the top of the film, with less intense signals at the corners. In the bottom of the film, the corners had higher intensity pDEMM signal than at the center of the film, consistent with the trends found for the polymerization data in Figure 4. Both the bottom and top of the film displayed similar ranges of pDEMM on the corners (or sides) of the film. Overall, more pDEMM was grafted on the pEAA-10-Na surface than the pEAA-3-Na surface, which is consistent with the increased number of initiating species. The pEAA-10 samples had more pDEMM on the surface than the base treated pEAA-10 and relatively little pDEMM was on the back side of the film. On the top surface of the film, more pDEMM was observed in the center, similar to the polymerization data.

Figure 5 displays the grafted pDEMM spatial heterogeneity (e.g., the amount of pDEMM on the film surfaces after washing non-grafted pDEMM with solvent). As expected, the LDPE-Na spectra exhibited only small amounts of pDEMM, because no imbedded initiator or chain transfer agent was present. Surprisingly, the pEAA-3-Na sample had the most even coverage of grafted pDEMM; however, pEAA-10-X samples had more pDEMM present. Conversely, the spectral signature of grafted pDEMM was seen on pEAA-10-X samples with and without base treatment on both sides of the film, with slightly higher intensities occurring on the pEAA-10 samples without base. The data in **Figure 5** both confirm the presence of pDEMM grafted to substrates with imbedded functional groups and a difference in heterogeneity based on concentration and mechanism (e.g., varying degrees of nucleophilicity and ability to act as a chain transfer agent).

DEM=M Transport during Surface Initiated Polymerization.

As seen in **Figure 6A**, the monomer droplet area increased during polymerization on nearly all substrates. To understand if monomer diffusion affected the grafting heterogeneity of pDEMM, the surface area of the monomer droplet was measured over time, and as the polymerization progressed, the visible area of the "polymerization front" (likely containing pDEMM and DEM=M) was quantified (**Figure 6B**). For all samples, the area increased the most during the first 4 hr. Of the base treated samples, LDPE-Na had the smallest increase in

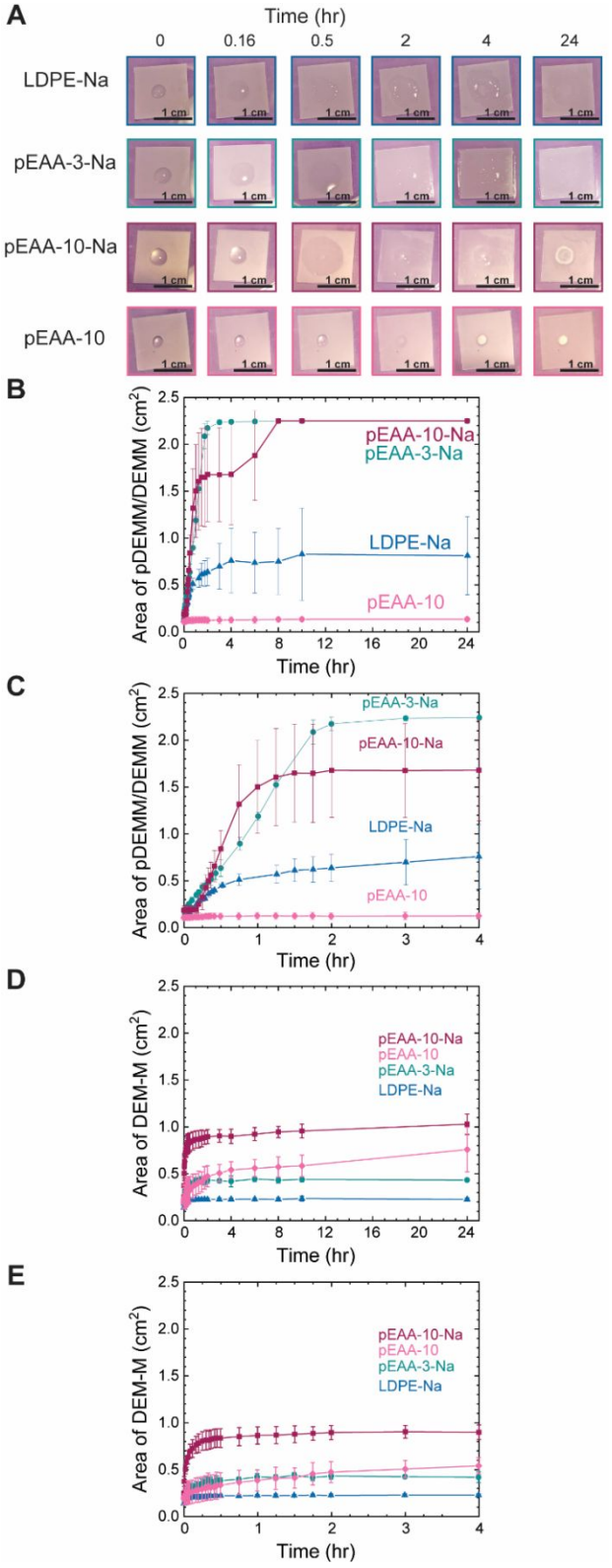

Figure 6. (A) Digital photographs of the movement of diethyl methylidene malonate on the surface of different substrates. The area of the diethyl methylidene malonate monomer and polymer on different substrates (LDPE-Na, pEAA-3-Na, pEAA-10-Na, and pEAA-10) was quantified over a (B) 24 hr polymerization period; (C) a magnified plot of the first 4 hr is also provided. The area of the non-reactive diethyl methylmalonate (control) was quantified on different substrates (LDPE-Na, pEAA-3-Na, pEAA-10-Na, and pEAA-10) over a (D) 24 hr period; (E) a magnified plot of the first 4 hr is also provided. (B-E) Mean and standard deviation are plotted for n=3.

area after 24 hr (36% coverage of the film), whereas pDEMM eventually covered the entire substrate on both pEAA-Na samples. As seen in **Figure 6C**, DEMM/pDEMM on pEAA-3-Na showed a continual and gradual increase in area (e.g., following a linear profile between 0-2 hr with an adjusted R^2 value >0.90). For pEAA-10-Na, there was an "induction period" in which the monomer front did not move, followed by the expansion of the polymerization front after ~10 min. In all samples, the slope between the induction period (10 min for pEAA-10-Na, 0 min for all other samples) and 30 min was linear (adjusted R^2 value >0.90). The slope of these lines was greatest for pEAA-10-Na (0.03 cm^2/min), followed by pEAA-3-Na (0.02 cm^2/min) and LDPE-Na (0.01 cm^2/min), with pEAA-10's slope nearly 2 orders of magnitude smaller than pEAA-10-Na's slope (0.0006 cm^2/min). The trend in the slopes of the base treated samples followed the amount of initiator in each sample. The difference in areal coverage between replicates could be due to surface heterogeneity (i.e., spatial clustering of acrylic acid salt or amorphous domains) or heterogenous diffusion. In general, our data suggests that the pDEMM front increased nearly linearly with lower initiator concentration and stepwise with higher initiator content.

In the case of pEAA-10, relatively little surface movement of pDEMM occurred but white, opaque polymer began to form at the surface between 1.25 and 4 hr. While no surface movement was observed on most replicate sets, at least one set of experiments showed a liquid polymer with some lateral movement after 24 hr polymerization, rather than an opaque polymer. Despite some heterogeneity between pEAA-10 replicates, the polymerization phenomena on pEAA-10 was markedly different than the polymerization on pEAA-10-Na. An induction time occurred in both pEAA-10-X samples; however, the pDEMM front grew past the area of the initial monomer droplet for pEAA-10-Na.

Effect of Wetting on DEM=M Surface Initiated Polymerization

We hypotheses that a combination of wetting and reactivity underlies the heterogenous polymerization and grafting phenomena, since the reaction front changes as a function of substrates with different initiators. The transport of a non-reactive control, diethyl methylmalonate (DEM-M), was measured to characterize the non-reactive aspects of the substrate-monomer interaction: DEM-M is nearly identical to diethyl methylidene malonate except for the double bond in the diethyl methylidene malonate monomer (DEM=M). As seen in **Figure 6D**, the final surface area of DEM-M was smaller than DEM=M for all substrates ($p<0.05$). The surface area of DEM-M increased minimally on LDPE-Na; on pEAA-3-Na and pEAA-10, the surface area of non-reactive DEM-M increased more than on LDPE-Na, and the two curves are similar. The final surface areas suggest that DEM-M has similar wetting behavior on pEAA-3-Na and pEAA-10. No induction time occurred on any of the substrates; all movement of DEM-M occurred immediately. The samples on pEAA-10-Na appeared less glossy at the end of 24 hr, likely due to less liquid DEM-M on the surface. This observation suggests that some of the DEM-M liquid diffused

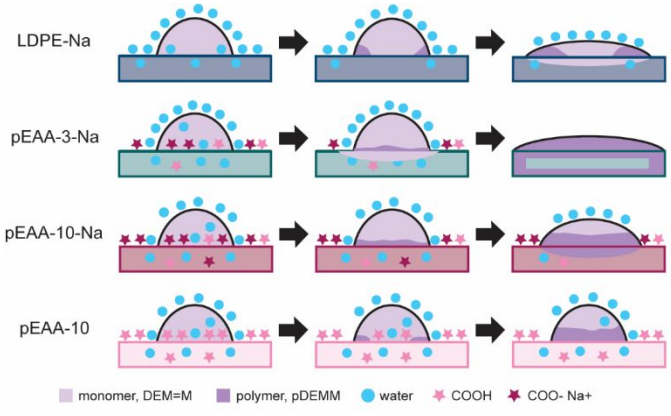

Scheme 2. Schematic displaying that the transport of DEM=M is mediated by the polymerization reaction. Moving across the row represents increasing time. See Schematic S1 for an expanded version of this schematic.

into the pEAA-10-Na substrate. pEAA-10-Na has the largest final area of DEM-M, suggesting that DEM-M has the most favorable wetting interaction with that surface.

By comparing the DEM-M and DEM=M data, we can conclude that simple wetting does not dominate the monomer transport and polymerization; otherwise, the monomer front progression would have matched the non-reactive liquid front progression. From the DEM-M data, some initial spreading (or movement on the surface of the substrate) occurred but reached equilibrium within the first 15 min. Furthermore, although DEM-M has similar wetting behavior on both pEAA-10 and pEAA-3-Na, the transport of DEM=M is markedly different on the two substrates, suggesting surface wettability is not the main factor dictating DEM=M transport. DEM=M may also diffuse into the substrate: as shown by the ATR-FTIR spectra, there was pDEMM on the back side of the films, and visually, there was less liquid DEM-M on the pEAA-10-Na substrates.

Proposed Reactive-Transport Mechanism of DEM=M Surface Initiated Polymerization.

We propose the following hypothesis to explain the reactive-transport behavior. When monomer is placed on the LDPE-Na substrate, anionic polymerization can occur from hydroxides in surface water; the air-interface acts as a source of additional hydroxides when the water condenses. At the edge of the monomer droplet, there is exposure to hydroxides on the surface and additional condensed water, and so the number of initiating species can out-compete the acid stabilizers (meant to slow or block spontaneous polymerization) in the monomer at the three-phase interface (air-substrate-monomer, vapor-solid-liquid) (**Scheme 2**, row 1). However, polymerization initiated by hydroxide anions is likely much slower (due to lower concentration) than polymerization by carboxylate salts. Additionally, any polymer which forms in the bulk from surface water acts as small particles, and will migrate to the interface (e.g., the coffee ring effect).[38,39] According to this literature, liquid and solutes move toward the pinned interface to replenish it as the liquid evaporates. Although we decreased evaporation by capping the substrate, some monomer will inevitably vaporize, which could be another driving force for the polymer and monomer to migrate toward the three-phase interface. Some of the monomer, which was previously in the bulk, is now exposed to additional hydroxide initiators at the three-phase interface. New polymerization occurs at the new interface on the outside of the previously created polymer, and monomer swells toward the new polymer, while any polymer "particles" formed in the bulk continue to move toward the new interface (**Scheme 2**, row 1, columns 2 and 3). This accounts for the rings observed in the LDPE-Na digital image, the large amount of pDEMM at the edges of the film, and the nearly non-existent pDEMM in the center where the droplet of monomer was initially placed.

In the case of pEAA-3-Na, another initiator is present on the surface, COO-Na+. We expected COO-Na+ to be more abundant, and a stronger initiating group, than the low concentration of hydroxide ions. Compared to the LDPE-Na substrate, the most likely initiation is on the surface and subsurface of the pEAA-3-Na substrate, where the COO-Na+ is located (**Scheme 2**, row 2 and column 2). However, bulk polymer particles will also be created by surface water or chain transfer, which will move toward the outer edge. The monomer can swell the polymer at the outer edge, increasing the visible area of the polymerization front, or in the z-direction (toward the bottom of the film). The presence of the more reactive COO-Na+ results in a faster and greater increase in area than the increase in surface area on LDPE-Na. There are relatively small amounts of COO-Na+, so the rate of the swelling and polymerization interactions may be balanced to give a nearly linear increase in the area of the polymerization front.

In the case of pEAA-10-Na, there are many more initiating groups on the surface compared to the pEAA-3-Na substrate, likely resulting in the growth of more pDEMM. The induction period may be due to the presence of more initiators, since the monomers continue to be consumed by the growing polymers tethered to the surface, rather than diffusing outward. The induction period may also be due to carboxylic acids associated with the carboxylate salts, since there are more total acids compared to pEAA-3-Na. According to the cyanoacrylate literature, the presence of weak acids slows the anionic polymerization of cyanoacrylates.[17,19,45]Carboxylic acids are unlikely to cause the induction time due to the large ratio of carboxylates to carboxylic acids. Another possibility is that the induction period is due to the low nucleophilicity of carboxylate salts, as reported by Reetz and coworkers for tetrabutyl ammonium salts of CH acidic compounds. They suggested that their observed induction period in the kinetic data was due to slower initiation than propagation.[20–22] Once the polymerizations are terminated, the monomer can further wet the grafted polymer.

In the case of the pEAA-10, both hydroxide and carboxylic acid are on the surface. The carboxylic acid groups could participate as initiators and as chain transfer agents, since the carboxylic acid can dissociate into a carboxylate with a hydrogen counterion in the presence of surface water. This carboxylate would be present at lower concentration (less absolute reactivity) than a carboxylate with sodium counterion. Additionally, the growing polymer chains can be terminated by

abstracting a hydrogen from COOH (e.g., chain transfer). We can envisage this long induction period as the monomers slowly reacting with the available initiators, and the rate of the chain growth is retarded. Again, this is supported by the cyanoacrylate literature, in which weak acids (COOH) slow the reaction rate.[45] The polymerization on the surface starts at the outer edge interface and progresses inwards, as more COOH groups begin to polymerize new chains (**Scheme 2**, row 4 and columns 2 and 3).

Once the polymers are terminated at the droplet-substrate interface, the monomers swell into the new polymers and continue to slowly diffuse outward and into the pEAA-10 film. While monomer movement is difficult to detect using a digital camera, and we could not capture the polymer front growing on pEAA-10, ATR-FTIR was able to detect pDEMM toward the films' corners. This may be due to a "precursor foot," which is normally detected in a spontaneously spreading liquid: a precursor foot is a thin (< 200 nm) film of liquid which spreads prior to the visible spreading of the droplet.[36] Additionally, we propose that if the monomer is diffusing into the film, that diffusion is slower in the pEAA-10 than the pEAA-10-Na sample. In the case of pEAA-10, for a new polymer chain to grow below the surface (or where there is no water present), a growing polymer with a reactive chain end must diffuse in and abstract a hydrogen. The diffusion process would become more difficult farther into the film, because the pDEMM would need to abstract nearly all COOH hydrogens of a layer before moving further, and the path is likely blocked by the previously polymerized pDEMM chains. This explanation is consistent with the small amount of grafted polymer found on the bottom of the pEAA-10 film: eventually the COOH cannot perform chain transfer because no growing chains are present. In the case of pEAA-10-Na, excess monomer can continue to swell down into the substrate.

Conclusions

In this work, we used ATR-FTIR to monitor the reaction of poly(diethyl methylidene malonate) on poly(ethylene-co-acrylic acid. We have demonstrated that the polymerization of pDEMM in ambient conditions from base treated pEAA substrates leads to both surface grafted polymer and free pDEMM. Interestingly, pEAA substrates without base treatment also demonstrated grafting of pDEMM; we hypothesize that carboxylic acid acts as both an initiator and chain transfer agent, and the polymers grown from initiation and after chain transfer are grafted to the surface. The heterogeneity of the surface grafting reaction was due to a combination of transport effects. Of the substrates studied, pEAA-3-Na demonstrated the most homogenous grafting of pDEMM, likely due to the favorable surface initiator concentration.

We also proposed a mechanism for our results based on the transport and reactivity for each substrate. On unfunctionalized LDPE, without surface bound initiators, DEMM polymerized at the three-phase interface from surface water, and through the coffee ring effect and monomer swelling, the polymer exhibited radial movement away from the initial droplet area. On pEAA-3-Na, DEMM steadily reacted with the available surface bound initiators and moved radially in a progressive fashion. In pEAA-10-Na, the abundance of surface initiators and the possible presence of associated weak acids resulted in an induction time, in which monomer stayed within the area of the initial droplet as the polymerization progressed; once the polymerization at the droplet-substrate interface was complete and saturated with monomer, the monomer moved toward new surface-bound initiators at the surface and sub-surface of the film. The surface-initiated polymerization on pEAA-10 occurred much more slowly, likely due to the slower initiation by weak acids and the chain transfer reaction. These processes resulted in a longer induction time for the main monomer droplet, observed as a static visible polymerization front during the 24-hr measurement. While we have demonstrated that surface initiated grafting of diethyl methylidene malonate is possible from acrylic acid based copolymers, for future studies, we suggest using a small amount of initiating groups in the substrate (similar to the pEAA-3-Na sample), and submerging the substrate in a bath of monomer diluted in a non-hydroscopic, polar, and aprotic solvent to promote optimal grafting. Systematically conducting these studies was beyond the scope of this work because polymerizing diethyl methylidene malonate from poly(ethylene acrylic acid) in the presence of solvents, yielded changes in wettability, differences in density, and the need to passivate glassware without inhibiting methylidene malonate polymerization, all of which required additional development and analysis. This study lays the groundwork to evaluate the effects of polymerization with multiple sources of initiation, chain transfer, and termination from polymeric surfaces.

Author Contributions

K.M.S.R. contributed to writing the original draft and editing the manuscript, as well as conceptualization, formal analysis, investigation, methodology, funding acquisition, and visualization. J.K. contributed to conceptualization, funding acquisition, editing, resources, and project administration. J.D.S contributed to conceptualization, funding acquisition, writing the original draft and editing, project administration, resources, and methodology.

Conflicts of interest

There are no conflicts to declare.

Acknowledgements

We thank Dr. Eric Hernandez and Mr. Louis Colaruotolo for helpful discussions. The authors thank Sirrus, Inc. for their support. We thank Entec for providing poly(ethylene-co-acrylic acid). K.M.S.R. thanks the Soft Materials for Life Sciences, a National Science Foundation-funded National Research Traineeship (DGE-1545399) for support.

References

1 P. Wyman, in *Coatings for Biomedical Applications*, ed. M. Driver, Woodhead Publishing Limited, Cambridge, UK, 2012, p. 376.
2 Rigoberto C. Advincula, William J. Brittain, Kenneth C. Caster and Jürgen Rühe, *Polymer Brushes: Synthesis, Characterization, Applications*, Wiley-VCH Verlag GmbH & Co. KGaA, Weinheim, Germany, 2004.
3 A. M. Chopra, M. Mehta, J. Bismuth, M. Shapiro, M. C. Fishbein, A. G. Bridges and H. V. Vinters, *Cardiovascular Pathology*, 2017, 30, 45–54.
4 *Lubricious Coating Separation from Intravascular Medical Devices: FDA Safety Communication*, Washington, D.C., 2015.
5 5 P.E. Guire, S.G. Dybjurj, M.W. Josephson, M.J. Swanson, US Pat., 5002582, 1989.
6 D.G. Swan, R.A. Amos, T.P. Everson, US Pat., 5714360A, 1998.
7 M.J. Swanson, R.A. Amos, D.G. Swan, G.W. Opperman, US Pat., 5942555A, 1996, 942, 376.
8 D.G. Swan, R.A. Amos, T.P. Everson, S.J. Chudzik, R.A. Chappa, S.M. Stucke, P.H. Duquette, US Pat., 7087658, 2006.
9 M. Militello, US Pat., 20170281831A1, 2017.
10 M. Huang, Y. Liu, G. Yang, J. Klier and J. D. Schiffman, *ACS Appl Polym Mater*, 2019, 1, 657–663.
11 United States, US8609885B2-, 2011.
12 B. P. Grady, *Polym Eng Sci*, 2008, 48, 1029–1051.
13 C. Zhang, N. Luo and D. E. Hirt, *Langmuir*, 2006, 22, 6851–6857.
14 A.G. Malofsky,T. Dey, J.M. Sullivan, Y. Chen, S. C. Wojciak, B.M. Malofsky, US Pat, 8884051, 2011.
15 M. Huang, Y. Liu, J. Klier and J. D. Schiffman, *Ind Eng Chem Res*, 2020, 59, 4542–4548.
16 P. Klemarczyk, *Polymer*, 1998, 39, 173–181.
17 P. Klemarczyk and J. Guthrie, in *Advances in Structural Adhesive Bonding*, Elsevier Inc., 2010, pp. 96–131.
18 D. C. Pepper, *Eur Polym J*, 1980, 16, 407–411.
19 E. F. Donnelly, D. S. Johnston, D. C. Pepper and D. J. Dunn, *Journal of Polymer Science: Polymer Letters Edition*, 1977, 15, 399–405.
20 M. T. Reetz, S. Hütte and R. Goddard, *J Am Chem Soc*, 1993, 115, 9339–9340.
21 M. T. Reetz, S. Hütte and R. Goddard, *J Phys Org Chem*, 1995, 8, 231–241.
22 M. T. Reetz, S. Hütte, H. M. Herzog and R. Goddard, *Macromol Symp*, 1996, 107, 209–217.
23 F. Ge, Q. Zhang and X. Wang, *Journal of Polymer Science*, 2021, 59, 764–774.
24 H.W. Coover, T. Kingsport, N.H. Shearer, E. Kodak, US Pat., 3221745, 1962.
25 J.-L De Keyser, J. H. Poupaert and P. Dumont, *J Pharm Sci*, 1991, 80, 67–70.
26 Z. Zhang, X. Zhu, J. Zhu, Z. Cheng and S. Zhu, *J Polym Sci A Polym Chem*, 2006, 44, 3343–3354.
27 A. E. Acar, M. B. Yağci and L. J. Mathias, *Macromolecules*, 2000, 33, 7700–7706.
28 A. K. Nanda, S. C. Hong and K. Matyjaszewski, *Macromol Chem Phys*, 2003, 204, 1151–1159.
29 D. Roy, J. T. Guthrie and S. Perrier, *Macromolecules*, 2005, 38, 10363–10372.
30 T. O'Haver, 2018.
31 C. A. Schneider, W. S. Rasband and K. W. Eliceiri, *Nat Methods*, 2012, 9, 671–675.
32 A. Zilkha, S. Barzakay and A. Ottolenghi, *J Polym Sci A*, 1963, 1, 1813–1837.
33 T. W. G. Solomons and C. B. Fryhle, *Organic Chemistry*, John Wiley & Sons, Inc., Hoboken, NJ, 9th edn., 2006.
34 S. R. Holmes-Farley, C. D. Bain and G. M. Whitesides, *Langmuir*, 1988, 4, 921–937.
35 S. R. Holmes-Farley, R. H. Reamey, T. J. McCarthy, J. Deutch and G. M. Whitesides, *Langmuir*, 1985, 1, 725–740.
36 J. C. Berg, *A Introduction to Interfaces and Colloids: the Bridge to Nanoscience*, World Scientific Publishing Co. Pte Ltd., 2010.
37 M. K. Chaudhury and A. Chaudhury, *Soft Matter*, 2005, 1, 431–435.
38 J. E. Forester, J. M. Sunkel and J. C. Berg, *J Appl Polym Sci*, 2001, 81, 1817–1825.
39 R. D. Deegan, O. Bakajin, T. F. Dupont, G. Huber, S. R. Nagel and T. A. Witten, *Nature 1997 389:6653*, 1997, 389, 827–829.
40 B. C. Smith, *Spectroscopy*, 2016, 31, 14–21.
41 A. Taubert and K. I. Winey, *Macromolecules*, 2002, 35, 7419–7426.
42 R. M. Walters, K. E. Sohn, K. I. Winey and R. J. Composto, *J Polym Sci B Polym Phys*, 2002, 40, 2833–2841.
43 B. C. Smith, *Spectroscopy*, 2021, 36, 9–15.
44 S. Savargaonkar, Slip Agents: Extended Performance Range for Polyolefin Films | Plastics Technology, https://www.ptonline.com/articles/slip-agents-extended-performance-range-for-polyolefin-films, (accessed 30 September 2021).
45 D. C. Pepper, *Polym J*, 1980, 12, 629–637.